processes

MDPI

Article

Experimental and CFD Investigation of the Spreading Dynamics and Fire Suppression Performance of Three Fire-Fighting Foams on Burning Fuel Surfaces

Yang Chen [1,2], Zhiming Bao [1,2,*], Xingfei Guo [3] and Zhao Dai [4,*]

[1] Key Laboratory of Fire Protection Technology for Industry and Public Building, Ministry of Emergency Management, Tianjin 300381, China; chenyang@tfri.com.cn
[2] Tianjin Fire Science and Technology Research Institute of MEM, Tianjin 300381, China
[3] School of Environmental Science and Engineering, Tiangong University, Tianjin 300387, China; guoxingfei@tiangong.edu.cn
[4] School of Chemical Engineering and Technology, Tiangong University, Tianjin 300387, China
* Correspondence: baozhiming@tfri.com.cn (Z.B.); daizhao@tiangong.edu.cn (Z.D.)

Abstract

Oil-pool fires involving liquid hydrocarbons are difficult to suppress and pose substantial economic risks. This study characterizes three widely used Class B fire suppressants through physical property measurements, cold oil-surface spreading tests, and burning oil-pool fire experiments, coupled with transient computational fluid dynamics (CFD) simulations in ANSYS Fluent. The results show that 3% aqueous film-forming foam (3% AFFF) and 3% alcohol-resistant aqueous film-forming foam (3% AFFF-AR) spread spontaneously on oil surfaces, whereas 3% fluoroprotein foam (3% FP) has a negative spreading coefficient and covers oil surfaces only through gravitational accumulation. Although 3% AFFF exhibits the fastest cold-state spreading, 3% AFFF-AR achieves the shortest fire-extinguishing time under combustion conditions because of its superior thermal stability and longer drainage time. In contrast, 3% FP shows the poorest fire-extinguishing performance. The CFD simulations capture the main temporal evolution of foam spreading and agree reasonably with experimental observations, particularly in the temporal consistency between simulated foam front propagation under the simplified elevated-temperature boundary condition and measured extinguishment times. Within the scope of the present simplified model and small-scale experiments, the results suggest that a positive spreading coefficient serves as a necessary but insufficient thermodynamic condition for effective foam spreading. Under high-temperature conditions, foam thermal stability critically influences the sustainability of spreading by resisting thermal degradation and bubble rupture, while drainage behavior and spreading kinetics modulate the coverage rate; collectively, these factors determine the overall fire suppression effectiveness under the tested conditions. These findings provide preliminary support for optimizing firefighting foam performance, pending validation under larger-scale and more fully resolved combustion scenarios.

Keywords: oil-pool fire; aqueous film-forming foam; spreading characteristics; fire-extinguishing performance; CFD simulation

Check for updates

Academic Editor: Alexander Penlidis

Received: 6 July 2026
Revised: 2 September 2026
Accepted: 7 September 2026
Published: 9 September 2026

Copyright: © 2026 by the authors. Licensee MDPI, Basel, Switzerland. This article is an open access article distributed under the terms and conditions of the Creative Commons Attribution (CC BY) license.

1. Introduction

Fire safety is essential for protecting life, property, and social and economic stability. According to the National Fire Protection Association (NFPA), liquid fuel fires account for a

significant proportion of Class B fire accidents in the petrochemical and aviation industries, causing billions of dollars in economic losses annually [1,2]. Foam-based suppression systems, including conventional low-expansion foam and compressed air foam, are critical for mitigating fire hazards in the petrochemical, aviation, and marine industries. These agents extinguish flames through two core mechanisms: heat absorption via internal water evaporation and oxygen exclusion by forming a continuous physical blanket atop liquid fuels. Five types of firefighting foams are commonly used in engineering: fluoroprotein foam (FP), aqueous film-forming foam (AFFF), film-forming fluoroprotein foam (FFFP), alcohol-resistant aqueous film-forming foam (AFFF-AR), and alcohol-resistant film-forming fluoroprotein foam (FFFP-AR) [1]. All of these products contain one or more fluorinated surfactants as key components for adapting to various fire conditions. Among them, FP, AFFF, and AFFF-AR are the three most widely applied and technically representative foams for industrial firefighting.

FP is one of the earliest industrialized fluorinated foams. Modified with fluorocarbon surfactants and based on traditional protein-based foam, FP exhibits excellent oil and burn-back resistance and has been widely applied in fixed fire-extinguishing systems for large-scale storage tanks. Nevertheless, limited by the rheological properties of their protein-based matrix, FPs have a relatively slow spreading rate and inferior rapid fire-suppression capacity when compared with synthetic foams. Previous FP optimizations focused on formula modification, and few comparative investigations have been carried out on spreading kinetics [3,4].

AFFF has been widely used in aviation fire-fighting to suppress Class B hydrocarbon fuel fires [5,6]. As a synthetic foam with low viscosity, AFFF can spread rapidly on most hydrocarbon fuel surfaces. Originally engineered for aviation kerosene fires, AFFF has demonstrated versatile suppression performance across multiple scenarios and can also mitigate Class A combustible solid fires [7]. As early as 1975, full-scale tests verified the applicability of AFFF in automatic water spray systems, further broadening its engineering application scope [8]. While a fire is being extinguished, a water film forms beneath the foam to cool the liquid fuel and inhibit the volatilization of combustible vapor [9]. The spreading and fire-suppression performance of AFFF is governed by the synergistic effect of fluorocarbon and hydrocarbon surfactants. The confidentiality of commercial formulas is an obstacle to conducting in-depth mechanism research [10]. With good fluidity and the ability to extinguish fires quickly, AFFF has dominated the market of Class B fire-extinguishing agents [11,12]. For large-area oil pools, the effective performance of AFFF relies on its ability to spread quickly over oil surfaces, which requires foam fluidity superior to pure liquids. In addition, due to the low surface tension of oil fuels, AFFF must maintain an even lower oil–foam interfacial tension to achieve a spreading coefficient (S) greater than zero [13]. However, conventional AFFF is only suitable for non-polar hydrocarbon fuels; on polar solvents such as alcohols, esters, and ketones, the aqueous foam film rapidly ruptures due to solvent-induced water extraction and bubble-matrix destabilization, resulting in immediate foam collapse and loss of surface coverage. Additionally, the perfluoroalkyl substances within AFFF raise concerns owing to their environmental persistence [14].

Alcohol-resistant aqueous film-forming foam (AFFF-AR) is a broad-spectrum suppressant developed by introducing high-molecular anti-alcohol components into the AFFF formula. It retains AFFF's ability to spread quickly and forms an isolating polymer membrane against polar fuels to avoid foam collapse. With the development of modern coal-chemical and fine-chemical industries, the risk of storing polar combustible liquids is continuously increasing; as a result, AFFF-AR has become an essential part of fire-protection systems in chemical plants [15]. Large-scale pool-fire experiments indicate that AFFF-AR presents much better spreading and fire-knockdown performance on polar fuels compared with

alcohol-resistant fluoroprotein foam under identical supply intensity, but its foam stability and burn-back resistance still require further improvement [16].

Although the process of forming aqueous films on liquid fuel surfaces remains unclear [17], there is scientific consensus on AFFF's fire-fighting mechanism: foam spreads to cover oil surfaces and extinguishes fires via cooling, surface blanketing and isolating oxygen [12]. Previous studies have investigated foam gas–liquid ratios, spreading kinetics, rheology, foam diffusion and foam drainage from multiple perspectives [13,17–19]. China's national standard GB 15308-2006 specifies performance requirements for the spreading behavior of AFFF suppressants ($S > 0$) [20]. Early studies established theoretical models for foam spreading at ambient temperature, laying a foundation for the quantitative characterization of spreading behavior; subsequent tests also confirmed that foam formula, expansion ratio and liquid film stability all directly affect the spreading rate [8,10]. Nevertheless, studies on foam fire-fighting systems revealed that $S > 0$ does not guarantee effective foam spreading, because S is fundamentally a thermodynamic equilibrium parameter rather than a kinetic coefficient. Derived solely from equilibrium interfacial tensions, S indicates only whether spontaneous spreading is energetically favorable, conveying no information about the rate at which spreading occurs. In practice, the actual spreading velocity and coverage efficiency are governed by kinetic factors such as foam viscosity, drainage behavior, and liquid film stability [21,22]. Quantitative investigations on foam spreading over oil surfaces under cold conditions have been conducted [17,22,23], and high-speed cameras can be used to directly record spreading processes to measure foam diffusion rates and the area covered [17]. However, the real-world foam fire-extinguishing process is extremely complex. High combustion temperatures, flame occlusion and thermal plume disturbances hinder the accurate representation of dynamic foam spreading, making it difficult to establish quantitative correlations between transient foam spreading and fire-extinguishing performance. Under cold conditions, high-speed cameras can directly record the dynamic spreading process of foam and precisely measure the foam front position, enabling the acquisition of diffusion rates and covered areas [15,16,19,20]. Under burning conditions, Persson et al. [24] used cameras to record foam front positions and developed a mathematical model to simulate foam spreading under both cold and burning conditions in the FOAMSPEX project, subsequently refining this model by incorporating viscous friction between the foam blanket and the underlying fuel [25]. However, these studies did not elaborate on how interferences such as flame luminosity and smoke obstruction were mitigated during image acquisition under burning conditions. Alternatively, Tan et al. [26] adopted an indirect approach in which the final foam position after extinguishment was recorded; the pool was then re-ignited and extinguished after the same pre-burning duration to facilitate flame-free spreading for high-precision camera recording, yielding an approximate measurement error of 5%. Nevertheless, continuous and precise measurement of dynamic foam spreading parameters, such as foam front velocity, under high-temperature combustion remains challenging owing to flame occlusion, smoke obstruction, and thermal plume disturbance. Consequently, most existing studies adopt total fire extinguishing time rather than foam diffusion rate as the core evaluation index [8,27,28], and direct quantitative correlations between transient foam spreading and fire extinguishing performance remain scarce.

Accordingly, this study investigates three typical firefighting foams (AFFF, AFFF-AR, and FP) through burning oil-pool fire tests coupled with computational fluid dynamics (CFD) simulations under elevated-temperature conditions. These conventional agents were selected not to promote legacy formulations facing environmental restrictions, but because their physical properties and fire-suppression behaviors have been extensively characterized, providing reliable benchmark data for model validation. Although previous studies

have investigated foam spreading under both cold and burning conditions [24–26], continuous and precise quantification of transient foam front velocity under high-temperature conditions remains challenging. By integrating burning oil-pool experiments with transient CFD simulations under high-temperature conditions, this study aims to establish a quantitative framework for evaluating foam spreading dynamics under elevated-temperature conditions. The primary objective of this study is to develop and validate a CFD simulation methodology for foam spreading dynamics under high-temperature conditions. The present work intentionally adopts a simplified treatment to focus on a specific and tractable question: whether the VOF-based multiphase flow solver, coupled with an experimentally calibrated elevated temperature, can satisfactorily capture the macroscopic spreading dynamics of firefighting foam on a high-temperature fuel surface. It should be emphasized that the validation of this framework focuses on the temporal consistency between simulated foam front advancement and experimentally observed extinguishment times, rather than on the fidelity of combustion simulation. Transient CFD simulations are utilized to complement experimental observations and compensate for observation blind zones induced by flame occlusion, and a multi-dimensional approach to evaluating foam suppression performance is proposed.

2. Materials and Methods

2.1. Materials

Three commercial foam concentrates were tested: 3% aqueous film-forming foam (3% AFFF, technical grade), 3% alcohol-resistant aqueous film-forming foam (3% AFFF-AR, technical grade), and 3% fluoroprotein foam (3% FP, technical grade). All foam concentrates were supplied by Jiangsu Suolong Fire Technology Co., Ltd. (Taizhou, China). The liquid fuel used in this study was industrial rubber solvent oil (a C6–C8 saturated alkane mixture; industrial grade), which was supplied by Sinopec Tianjin Branch (Tianjin, China). Its physical properties at 20 °C were as follows: density of 0.680 g/cm^3, kinematic viscosity of 0.60 mm^2/s, surface tension of 21.44 mN/m, and closed-cup flash point of −4 °C. The distillation range was 80–120 °C.

2.2. Cold Foam Spreading Experiment

The foam-spreading test was carried out in a rectangular channel with a length of 4.5 m, width of 1 m, and height of 0.25 m (Figure 1). A total of 90 L of tap water was injected to form a 2 cm thick water layer, and then 90 L of solvent oil was added to form a 2 cm thick oil layer. The foam solution flow rate of 11.4 L/min was adopted as the experimental operating condition in this study. The foam nozzle was aligned to the middle of the baffle, and a high-definition camera was used to record the entire spreading process once the foam discharge stabilized.

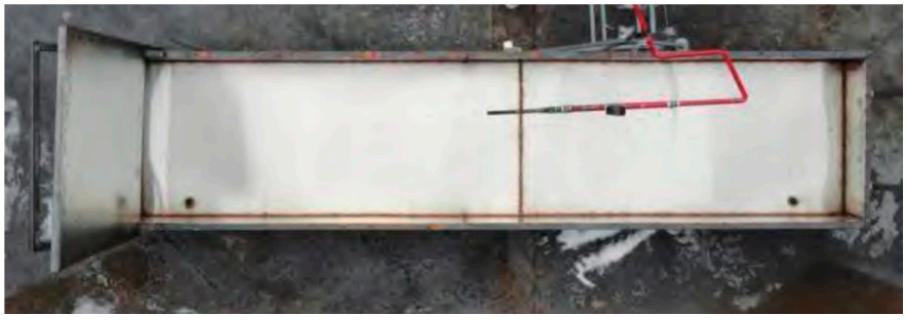


Figure 1. Schematic of foam-spreading experimental device.

Foam viscosity was measured using a Brookfield R/S+CC rheometer (AMETEK Brookfield, Middleboro, MA, USA) equipped with a paddle rotor, and the rheological parameters were obtained using Rheo 3000 V1.0 (2007) software. The surface tension and oil–water interfacial tension of the three foam solutions were measured using a K100C automatic surface tensiometer (KRÜSS GmbH, Hamburg, Germany) with the Wilhelmy plate method [29]. All experiments were performed in triplicate.

The film-forming conditions of a foam fire-extinguishing agent on the surface of water-insoluble fuel depend on the surface tensions of the fuel and foam solution and the interfacial tension between the fuel and foam solution, which satisfies Equation (1):

$$S = r_{fuel} - r_{foam} - r_i > 0 \quad (1)$$

where S is the spreading coefficient, mN/m; r_{fuel} is the surface tension of the fuel, mN/m; r_{foam} is the surface tension of the foam solution, mN/m; and r_i is the interfacial tension between the fuel and foam solution, mN/m.

2.3. Fire-Extinguishing Experiment

A slow foam discharge mode was adopted, with a foam flow rate of 11.4 L/min. The solvent oil layer was 2 cm thick with 90 L of water underneath. The pre-combustion duration was fixed at 60 s, and foam was continuously supplied until the flame was completely extinguished. A video camera was positioned above the oil pool to record the entire foam-spreading, flame-suppressing, and fire-extinguishing process. It should be noted that the fire-extinguishing experiments were conducted once for each foam agent because replicate burning tests involving large-scale pool fires pose high safety risks and significant environmental hazards. Consequently, the reported extinguishment times represent single-trial observations rather than statistically averaged values. In the burning experiments, the oil-pool temperature was monitored as a key parameter affecting foam viscosity and spreading behavior. The pool fire temperature reached approximately 873 K (600 °C) at steady state after the 60 s pre-combustion period, and remained in the range of 600–700 °C throughout the foam discharge and extinguishment process. This temperature evolution is consistent with extinguishment time-temperature profiles reported in the literature for similar pool-fire suppression scenarios [8,26,30].

2.4. CFD Numerical Simulation Method

Based on the geometric size of the rectangular experimental pool, a three-dimensional geometric model with dimensions of 5.75 m × 1.25 m × 1.00 m was established using ANSYS FLUENT 2021R2 (ANSYS, Inc., Canonsburg, PA, USA). The overall computational domain was enlarged. This arrangement avoided artificial confinement of the fire plume, permitted unobstructed air entrainment, and prevented a high-temperature plume from encountering domain boundaries. The extended outer boundaries were defined as a pressure outlet for ambient atmospheric conditions, while the oil-pool walls were considered no-slip wall boundaries to avoid distorted thermal fields and unreliable foam-spreading predictions. Within the computational domain, the 3D geometric model and hexahedral structured mesh were generated using ANSYS ICEM CFD 2021R2, with a total cell count of approximately 600,000 (Figure 2).

Mesh-independence verification was completed prior to formal calculation: three groups of meshes with different densities were tested, and the spreading coverage of 3% AFFF foam under the elevated-temperature boundary condition at t = 180 s was selected as the monitoring parameter (Table 1). The relative deviations in foam-spreading coverage between the different meshes were all less than 2%, confirming mesh independence.

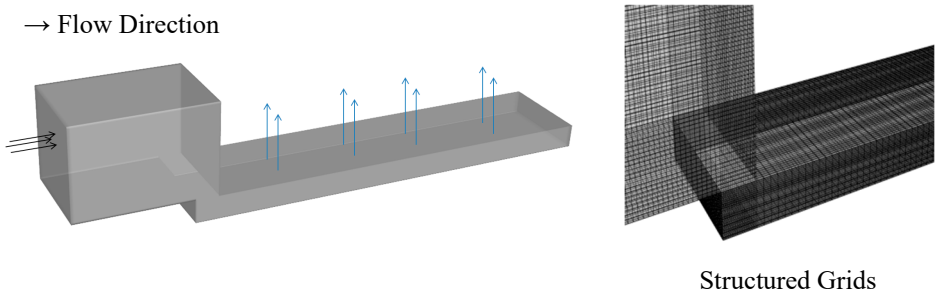


Figure 2. The 3D geometric model and structured hexahedral mesh of the oil-pool computational domain. Note: The black arrows denote the foam inlet, while the blue arrows represent the foam outlet.

Table 1. Mesh-independence verification based on the percentage of the oil-pool length covered by 3% AFFF foam under the elevated-temperature boundary condition.

Cell Count	Monitoring Time (s)	Foam Area Coverage (%)	Relative Deviation (%)
300,000	180	81.64	1.97
600,000	180	80.06	-
900,000	180	78.55	1.89

The Volume of Fluid (VOF) multiphase model was adopted to capture the evolution of the gas–liquid–foam interface under transient elevated-temperature boundary conditions. Different foam-agent physical parameters were imported into the computational domain to compare fire-extinguishing performance.

Boundary conditions were set based on experimental operating conditions: the inlet was defined as a velocity inlet. The volume fraction of the foam phase was set to 1 at the velocity inlet boundary, with a constant volumetric flow rate of 11.4 L/min and a temperature of 293.15 K; the outlet was specified as an outflow boundary. Since the actual fuel layer height at the bottom of the combustion tank was 4 cm, the volume fraction of the fuel phase was set to 1 in the region 4 cm above the tank bottom. The foam was treated as a homogeneous equivalent fluid (a single mixed phase), and no gas-phase reaction zone was included. The density and viscosity of the foam were determined from the physical properties measured from stable foam at room temperature. The fuel temperature in the oil-pool region was set to 873.15 K (600 °C), corresponding to the measured pool fire temperature at steady state after 60 s of pre-combustion. The temperature represents the operative thermal condition during foam spreading rather than the theoretical maximum combustion temperature. The sidewall temperature was not measured during the experiments and the sidewalls of the experimental pool were not explicitly modeled as transient heated surfaces; instead, they were treated as no-slip solid boundaries within the overall thermal environment. This simplification does not resolve localized wall heating or its potential destructive effect on the foam, which is acknowledged as a limitation of the present model. Consequently, the validation of this model focuses on the temporal agreement between the simulated foam front propagation and the measured fire-extinguishing times, rather than on the fidelity of combustion simulation. A transient simulation was employed for calculation with a time step of 0.1 s. The 0.1 s time step adequately resolved the hundred-second-scale foam-spreading dynamics while balancing numerical stability and computational cost; iterative convergence was achieved at each time step. The PRESTO! scheme was used for pressure interpolation, and the first-order upwind scheme was adopted for momentum discretization. The coupled algorithm was selected for pressure–velocity coupling, while the first-order upwind scheme was applied to all other conservation equations. The total physical calculation time was set to 700 s. The computation was considered converged

when the residuals of all flow variables dropped below 10^{-4} and the residuals of species mass fractions fell below 10^{-6}.

3. Results and Discussion

3.1. Fundamental Physical Properties of Fire-Fighting Foams

Liquid fuel oils exhibited low surface tension, which varied significantly with temperature. According to liquid–liquid spreading theory, fire-fighting foams must possess low surface and oil–water interfacial tension to achieve spontaneous spreading, film formation, oxygen isolation, and suppression of oil vapor volatilization on burning fuel surfaces [17,21]. In this study, quantitative measurements of the expansion ratio, 25% drainage time, yield stress, surface tension, and oil–water interfacial tension were conducted for the three foam concentrates at ambient temperature; the measured physical parameters are summarized in Table 2.

Table 2. Measured physical properties of three tested fire-fighting foams.

Foam Agent	Foam Expansion Multiple	25% Drainage Time (s)	Yield Stress (Pa)	Surface Tension (mN/m)	Oil–Water Interfacial Tension (mN/m)
3% AFFF	7.98 ± 0.12	131 ± 0.13	1.36 ± 0.12	16.31 ± 0.08	2.061 ± 0.11
3% AFFF-AR	8.36 ± 0.09	415 ± 0.12	1.46 ± 0.11	15.85 ± 0.12	1.756 ± 0.09
3% FP	6.79 ± 0.10	189 ± 0.10	2.89 ± 0.04	21.22 ± 0.10	6.436 ± 0.12

Note: Values are presented as mean ± half-range (n = 3).

The surface tension of the industrial rubber solvent oil is 21.44 mN/m. The calculated spreading coefficients were +3.07 mN/m for the 3% AFFF, +3.83 mN/m for the 3% AFFF-AR, and −6.22 mN/m for the 3% FP, indicating that only the first two agents possess the thermodynamic driving force for spontaneous spreading over the fuel surface, while the 3% FP must rely entirely on gravitational accumulation [30]. This trend is consistent with prior interfacial tension characterizations of various fluorinated fire-fighting foams [17,19], and fundamental interfacial chemistry investigations have further confirmed that the tension difference between two immiscible liquids is the core thermodynamic prerequisite for spontaneous foam spreading [22].

The 25% drainage time serves as a critical metric reflecting foam skeleton stability and water retention capacity [19]. The 25% drainage time of the 3% AFFF-AR is remarkably longer than those of the other two foams, indicating superior water retention and intact liquid film performance. The 3% AFFF and 3% FP presented comparable drainage durations and relatively weak structural stability overall. Although rapid liquid drainage releases water to cool oil surfaces instantaneously, it accelerates foam volume loss and drastically reduces the sustained coverage capacity required for large oil pools. Established kinetic foam drainage models demonstrate that the drainage rate directly controls the duration of complete foam coverage [19]; supplementary thermal aging characterizations further verify that foams with extended drainage times display substantially reduced liquid film rupture rates in high-temperature environments [5].

3.2. Cold-Surface Spreading Characteristics of Fire-Fighting Foams

Flame-free cold oil-surface spreading experiments were carried out to eliminate thermal interference induced by combustion. Temporal variations in foam spreading rates for all three agents are illustrated in Figure 3. Despite having similar baseline physical properties (surface tension, oil–water interfacial tension and yield stress), the 3% AFFF and 3% AFFF-AR's cold-surface spreading rates differed substantially, mainly originating from

divergent drainage and film-forming kinetics. The 3% AFFF underwent rapid drainage and quickly formed a continuous lubricating water film on the oil surface, which accelerated the advancement of foam fronts driven by interfacial tension, thus achieving optimal spreading performance under ambient cold conditions. For the 3% FP, the negative spreading coefficient (−6.22 mN/m) eliminated the spontaneous spreading capacity provided by interfacial tension gradients, resulting in persistent high spreading resistance and low propagation velocity. Quantitative full-process monitoring of cold foam spreading via high-speed cameras proved that AFFF relies on quickly draining water films to accelerate surface propagation [19]. This conclusion is consistent with the present cold-test results, in which 3% AFFF exhibited the maximum spreading rate despite having interfacial tension comparable to that of 3% AFFF-AR, indicating that spreading kinetics are controlled by drainage behavior rather than by the spreading coefficient alone [22,31].

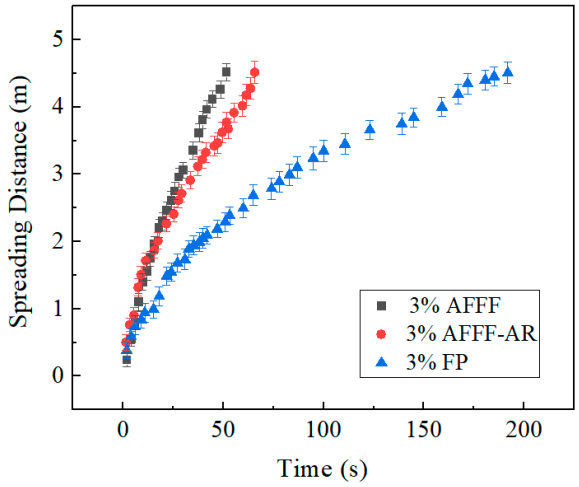


Figure 3. Spreading rates of three fire-fighting foams on a cold fuel surface.

3.3. Spreading and Fire-Extinguishing Characteristics of Foams on Burning Oil Surface

To simulate real-world oil-pool fire conditions, burning oil surface-spreading and fire-extinguishing tests were conducted with uniform foam flow rate control, oil layer thickness, pre-burning time, and other parameters. ANSYS Fluent CFD simulation was used to reproduce the microscopic flow characteristics of foam spreading under high temperature, compensating for the observation blind zone caused by flame shielding and establishing a correlation between the macroscopic fire-extinguishing phenomenon and microscopic spreading mechanism.

3.3.1. Spreading and Fire-Extinguishing Performance of 3% AFFF

The 3% AFFF delivered the best spreading performance under cold ambient conditions, yet its spreading and fire-extinguishing efficiency decreased significantly in a high-temperature combustion environment. After foam injection, the foam front advanced slowly toward the pool center, covering most regions of the oil pool at 180 s and fully extinguishing the flames only at 230 s (Figure 4). Intense thermal radiation and thermal plumes generated by combustion continuously impacted foam skeletons, accelerating bubble rupture and liquid drainage and destroying the integral foam blanket. Elevated temperatures also altered the interfacial tension-matching state between the fuel oil and foam, further weakening the driving force for spontaneous spreading. Although the 3% AFFF showed favorable thermodynamic spreading characteristics at room temperature, its insufficient high-temperature structural stability prevented it from maintaining continuous

oxygen-isolating water films in the long term, eventually extending the time required for full oil-surface coverage and complete flame extinction.

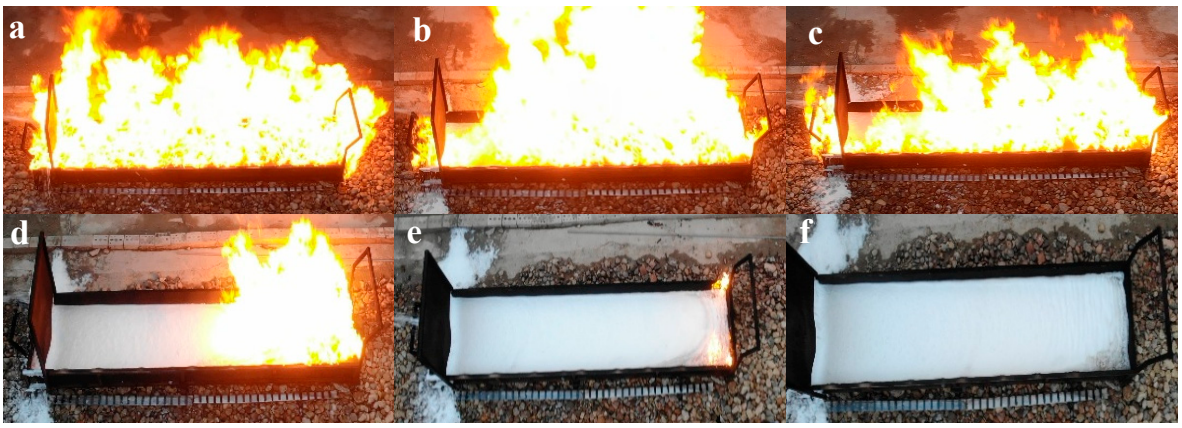


Figure 4. Time-lapse experimental images of the fire-extinguishing process of 3% AFFF foam: (**a**) 0 s; (**b**) 30 s; (**c**) 60 s; (**d**) 120 s; (**e**) 180 s; (**f**) 230 s.

Figure 5 shows the simulated foam front positions at t = 30, 60, 120, 180, and 230 s after the initiation of foam discharge, reaching approximately 42%, 62%, 91%, 99%, and 100% of the pool length, respectively. These simulated results are reasonably consistent with the fire-extinguishing observations in the fire-suppression experiments (Figure 4), indicating that the CFD model satisfactorily captured the foam front propagation speed. The good agreement regarding temporal evolution suggests that oil surface coverage, driven by foam front advancement, is the primary fire suppression mechanism in this scenario.

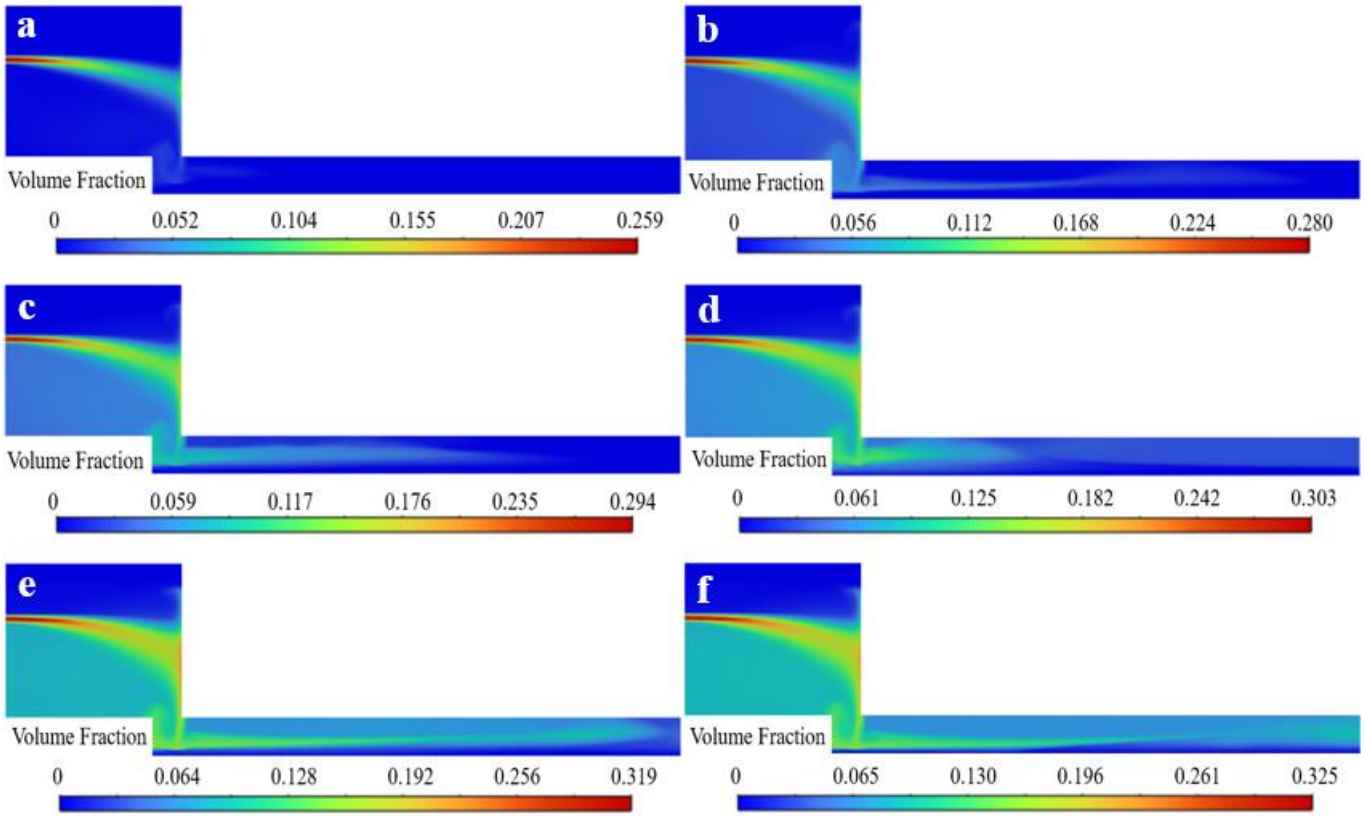


Figure 5. Contour nephograms of foam volume fraction for simulated spreading process of 3% AFFF foam on fuel oil surface under elevated-temperature conditions: (**a**) 0 s; (**b**) 30 s; (**c**) 60 s; (**d**) 120 s; (**e**) 180 s; (**f**) 230 s.

However, continuous measurement of the foam surface coverage area over time was not achievable in the burning experiments because flame luminosity and smoke significantly interfered with optical camera imaging. Consequently, a direct quantitative comparison of surface coverage area versus time could not be established. The comparison of foam front positions at specific time points offers a preliminary validation of the simulation's reliability.

3.3.2. Spreading and Fire-Extinguishing Performance of 3% AFFF-AR

The 3% AFFF-AR's fire-extinguishing process is shown in Figure 6. Compared with the 3% AFFF, the 3% AFFF-AR presented a slightly slower cold spreading rate but much better comprehensive performance under combustion conditions. It completely covered the oil surface at 120 s and completely extinguished the fire at 180 s. This foam's lower surface and oil–water interfacial tension, sufficient thermodynamic spreading characteristics, and longer 25% drainage time greatly improve its structural stability and high-temperature resistance.

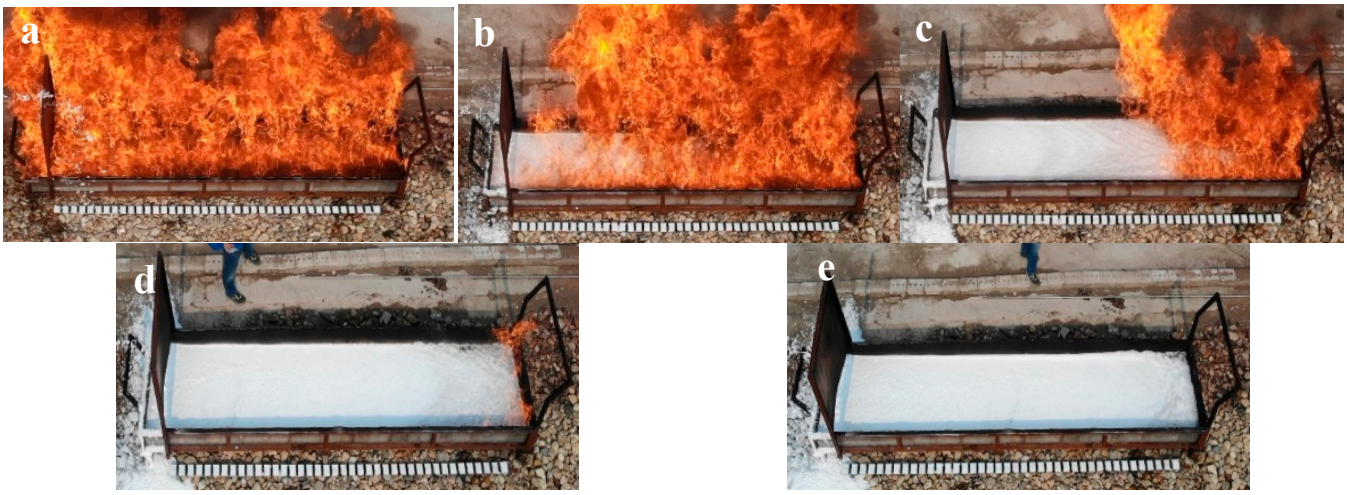


Figure 6. Time-lapse experimental images of the fire-extinguishing process of 3% AFFF-AR foam: (**a**) 0 s; (**b**) 30 s; (**c**) 60 s; (**d**) 120 s; (**e**) 180 s.

When exposed to thermal radiation from combustion, AFFF-AR foam resists rapid defoaming and excessive liquid drainage, rapidly forming dense continuous water films and foam blankets over oil surfaces. These layered structures block oxygen diffusion toward combustion zones, while sustained mild drainage absorbs heat to cool oil surfaces and suppress the volatilization of flammable fuel vapor. Alcohol-resistant modified surfactant components endow the foam with enhanced resistance to high-temperature disturbance and airflow-induced bubble fragmentation. Collectively, the 3% AFFF-AR's balanced spreading kinetics, foam thermal stability, and oxygen-isolating cooling capacity make it the most efficient fire-extinguishing agent among the three foams tested. The simulated AFFF-AR foam front positions (Figure 7) at t = 30, 120, and 180 s after the initiation of foam discharge reached approximately 60%, 83% and 100% of the pool length, respectively. These results are consistent with the fire-extinguishing test observations (Figure 6). These simulations confirm that AFFF-AR foam fronts advance faster and retain higher foam volume fractions under identical conditions, with far less structural attenuation under high temperatures compared with conventional AFFF.

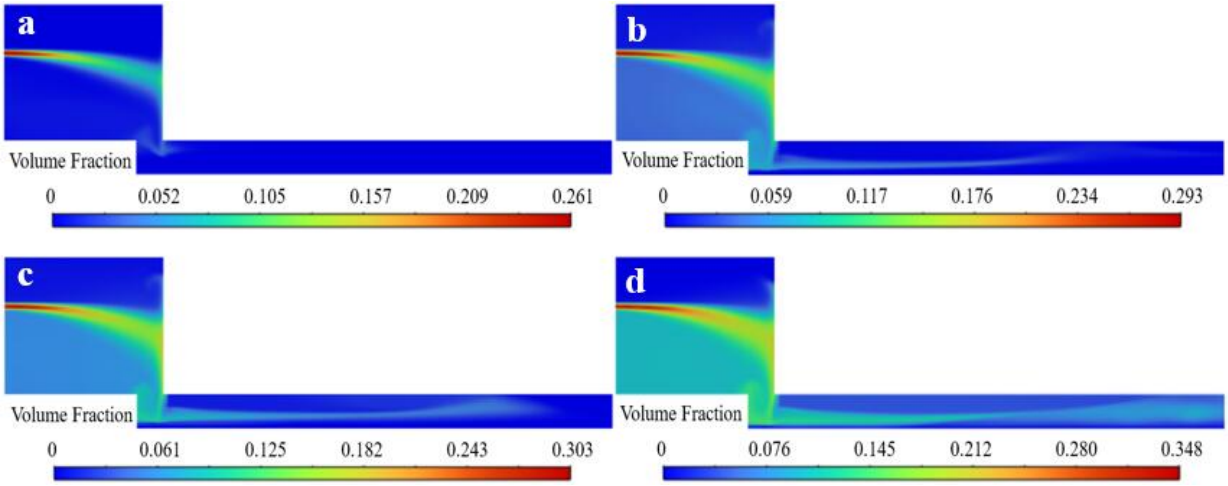


Figure 7. Contour nephograms of foam volume fraction for simulated spreading of 3% AFFF-AR foam on a fuel oil surface under elevated-temperature conditions: (**a**) 0 s; (**b**) 30 s; (**c**) 120 s; (**d**) 180 s.

3.3.3. Spreading and Fire-Extinguishing Performance of 3% FP

The 3% FP required 670 s to fully extinguish the oil-pool flames, which is 2.91 times the extinction time of the 3% AFFF (230 s) and 3.72 times that of the 3% AFFF-AR (180 s), demonstrating extremely inferior fire-extinguishing efficiency (Figure 8). Physical property testing revealed that the surface tension of the 3% FP was close to that of solvent fuel oil, yielding a negative spreading coefficient and eliminating interfacial tension-driven spontaneous spreading capacity. The foam can only cover oil surfaces slowly, relying on gravitational accumulation, and its high yield stress further impairs fluidity and spreading velocity. Although it has a moderate drainage capacity to supply water for oil surface cooling, severely deficient spreading kinetics cause foam fronts to propagate far slower than flame spreading and thermal destruction rates. Continuous high-temperature erosion breaks foam bubbles and dissipates foam blankets, preventing the formation of stable continuous oxygen-isolating water films; flames can only be suppressed gradually via long-term foam accumulation.

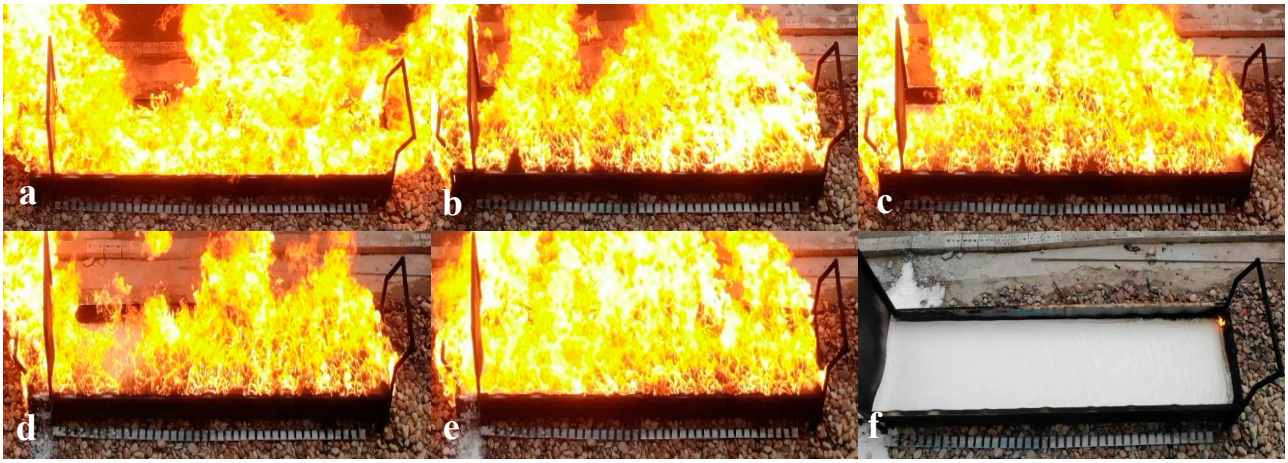


Figure 8. Time-lapse experimental images of the fire-extinguishing process of 3% FP foam: (**a**) 0 s; (**b**) 30 s; (**c**) 60 s; (**d**) 120 s; (**e**) 180 s; (**f**) 670 s.

CFD numerical simulations (Figure 9) showed that the 3% FP foam front advances slowly. At t = 30, 60, 120, 180, and 670 s after the start of foam discharge, the simulated foam front reached approximately 5%, 22%, 41%, 91%, and 100% of the pool length, respectively. These results are consistent with the fire suppression observations (Figure 8). This indicates

that FP foam covers a far smaller oil area at identical time points and requires substantially more time to fully cover the oil pool, which explains the underlying mechanism behind its excessively long fire suppression time from a microscale flow field perspective.

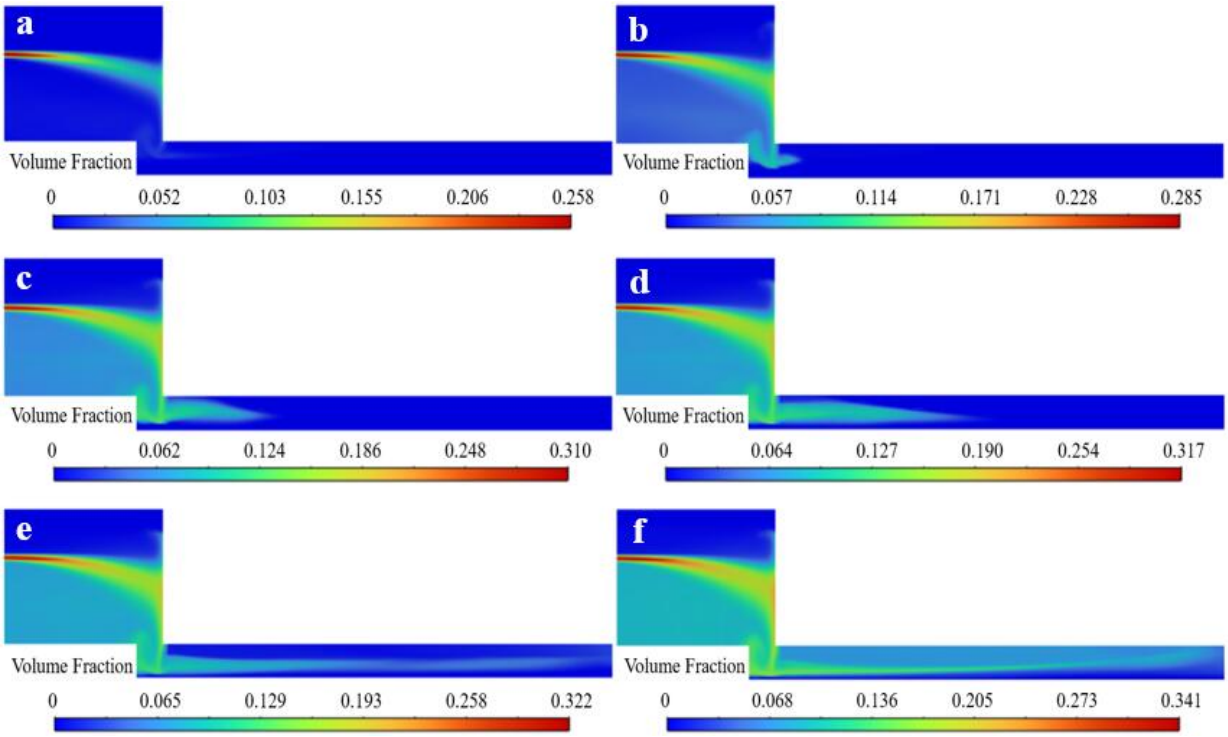


Figure 9. Contour nephograms of foam volume fraction for simulated spreading process of 3% FP foam on fuel oil surface under elevated-temperature conditions: (**a**) 0 s; (**b**) 30 s; (**c**) 60 s; (**d**) 120 s; (**e**) 180 s; (**f**) 670 s.

4. Conclusions

Differences in inherent physical properties result in divergent spreading behaviors among firefighting foams on oil surfaces. 3% AFFF and 3% AFFF-AR possess low surface and oil–water interfacial tension, which supports spontaneous spreading over hydrocarbon fuels. In contrast, 3% FP exhibits interfacial tension values close to those of the test solvent oil and a negative spreading coefficient; consequently, it relies entirely on gravitational accumulation to achieve oil-surface coverage, and does so slowly. Rheological discrepancies among the three foam samples remain limited. Within the constraints of the present simplified model and small-scale experiments, the results indicate that the degree of oil–water interfacial tension matching and foam drainage stability strongly influence spreading dynamics and fire-extinguishing performance under the tested conditions. A clear mismatch exists between cold-state foam spreading performance and actual fire knockdown efficiency under high-temperature combustion conditions. Although 3% AFFF spreads fastest in flame-free cold tests, it suffers from poor structural stability under thermal radiation, prolonging flame extinction time. Benefiting from superior thermal tolerance and persistent film-forming capacity, 3% AFFF-AR maintains continuous, intact foam blankets on burning oil surfaces and demonstrates optimal fire-extinguishing efficiency among all agents tested. Lacking spontaneous spreading driving force and prone to rapid structural attenuation under high temperatures, 3% FP requires an extremely long time to extinguish pool fires and fails to meet the rapid suppression requirements of large-area liquid fuel fires. Transient CFD simulations based on the VOF multiphase framework, under the simplified thermal boundary conditions employed here, capture the main evolutionary trends of foam spreading on high-temperature oil surfaces, and numerical predictions show

reasonable agreement with the small-scale experimental observations, thereby helping to compensate for observation blind zones generated by flame occlusion in conventional experimental tests. The model presented in this study is primarily intended to resolve macroscopic spreading dynamics rather than detailed combustion chemistry or microscale foam-degradation processes.

Several limitations of this work should be acknowledged. First, the fire-extinguishing experiments were conducted once for each foam agent because replicate burning tests involving large-scale pool fires pose high safety risks and significant environmental hazards; consequently, the reported extinguishment times (230 s for 3% AFFF, 180 s for 3% AFFF-AR, and 670 s for 3% FP) represent single-trial observations rather than statistically averaged values. Second, the experiments were conducted in a small-scale rectangular pool (4.5 m × 1 m × 0.25 m) due to laboratory space constraints and combustion safety regulations. Consequently, sidewall confinement significantly retarded foam spreading near the boundaries, and the radiative feedback, air entrainment, and flame dynamics differ from those in full-scale fires; thus, direct extrapolation of the results to engineering-scale applications requires caution. Third, although the CFD model replicated the no-slip wall boundaries and captured the wall-induced foam accumulation, the simulations employed a simplified combustion treatment—using an elevated ambient temperature (873.15 K) rather than fully coupled combustion chemistry, heat release, fuel vaporization, or thermal radiation—which precluded detailed resolution of flame–foam interactions. Additionally, the sidewall temperature was not measured during the experiments and was not accounted for in the simulations; instead, the sidewalls were treated as no-slip solid boundaries within the overall thermal environment. The reasonable agreement between simulation and experiment is achieved because the model captures the dominant macroscopic spreading dynamics and the overall thermal resistance of the high-temperature environment, rather than resolving localized wall–foam interactions. Fourth, microscopic phenomena, including foam drainage, bubble rupture, and thermal degradation, were not explicitly resolved; instead, their macroscopic effects were accounted for indirectly through effective foam properties and the built-in temperature–fluid coupling algorithm. Finally, quantitative experimental validation of surface coverage area was hindered by flame luminosity and smoke obstruction, restricting the validation to semi-quantitative comparisons of foam front positions and extinguishment times.

Author Contributions: Conceptualization, Y.C. and Z.B.; methodology and software, X.G.; validation, Y.C. and Z.D.; formal analysis, Y.C.; investigation, Y.C.; resources, Z.B. and Z.D.; data curation, Y.C.; writing—original draft preparation, Y.C.; writing—review and editing, Z.B. and Z.D.; visualization, X.G.; supervision, project administration and funding acquisition, Z.D. All authors have read and agreed to the published version of the manuscript.

Funding: This research was funded by Open Foundation of Key Laboratory of Fire Protection Technology for Industry and Public Building, Ministry of Emergency Management (Grant No: 2023KLIB04).

Data Availability Statement: The data that support the findings of this study are available from the corresponding author upon reasonable request.

Conflicts of Interest: The authors declare no conflicts of interest.

References

1. Malik, P.; Nandini, D.; Tripathi, B.P. Firefighting aqueous film forming foam composition, properties and toxicity: A review. *Environ. Chem. Lett.* **2024**, *22*, 2013–2033. [CrossRef]
2. Wan, B.; Parker, T.; Wang, Q. Thermal modeling for supporting firefighting and emergency response planning. *Process Saf. Prog.* **2023**, *42*, 105–115. [CrossRef]

3. Pabon, M.; Corpart, J.M. Fluorinated surfactants: Synthesis, properties, effluent treatment. *J. Fluor. Chem.* **2002**, *114*, 149–156. [CrossRef]
4. Peshoria, S.; Nandini, D.; Tanwar, R.K.; Narang, R. Short-chain and long-chain fluorosurfactants in firefighting foam: A review. *Environ. Chem. Lett.* **2020**, *18*, 1277–1300. [CrossRef]
5. Zhao, M.; Ni, X.M.; Zhang, S.G.; Cao, W.; Guan, Y.; Liang, C.J.; Wang, X.S.; Zhang, H.P. Improving the performance of fluoroprotein foam in extinguishing gasoline pool fires. *Fire Mater.* **2016**, *40*, 261–272. [CrossRef]
6. Wang, K.; Yue, Q.; Zhang, J.; Chen, P.; Wang, Z.; Wang, W.; Zhou, Y.; Zhou, B. Temperature effects of the artificial accelerated ageing of aqueous film-forming foam agent on the foam structural stability. *Therm. Sci. Eng. Prog.* **2025**, *64*, 103819. [CrossRef]
7. Rie, D.H.; Lee, J.W.; Kim, S. Class B fire-extinguishing performance evaluation of a compressed air foam system at different air-to-aqueous foam solution mixing ratios. *Appl. Sci.* **2016**, *6*, 191. [CrossRef]
8. Yan, L.; Wang, N.; Guan, J.; Wei, Z.; Xiao, Q.; Xu, Z. Comparative study of the suppression behavior and fire-extinguishing mechanism of compressed-gas aqueous film-forming foam in diesel pool fires. *Fire* **2023**, *6*, 269. [CrossRef]
9. Burford, R.R. The use of AFFF in sprinkler systems. *Fire Technol.* **1976**, *11*, 5–17. [CrossRef]
10. Li, H.; Yu, X.Y.; Qiu, K.; Yu, X.; Lu, S.X. Enhanced fire-fighting performance of aqueous film-forming foam (AFFF) by tuning bubble size and expansion ratio with kenics static mixers. *Fire Saf. J.* **2024**, *144*, 104117. [CrossRef]
11. Meissner, E.; Twardochleb, B.; Milchert, E.; Wróblewska, A.; Szymanowski, J. Estimation of foam forming properties and surface tension of fire-extinguishing agents. *Tenside Surfactants Deterg.* **2003**, *40*, 353–360. [CrossRef]
12. Xu, Z.S.; Guo, X.; Yan, L.; Kang, W.D. Fire-extinguishing performance and mechanism of aqueous film-forming foam in diesel pool fire. *Case Stud. Therm. Eng.* **2020**, *17*, 100578. [CrossRef]
13. Woodman, A.L.; Richter, H.P.; Adicoff, A.; Gordon, A.S. AFFF spreading properties at elevated temperatures. *Fire Technol.* **1978**, *14*, 265–272. [CrossRef]
14. Moody, C.A.; Field, J.A. Perfluorinated surfactants and the environmental implications of their use in fire-fighting foams. *Environ. Sci. Technol.* **2000**, *34*, 3864–3870. [CrossRef]
15. Kaller, M.; Van Bortel, G.; Engels, T.; Thierens, R.; Fachinger, J. An evaluation of the firefighting performance of alcohol-resistant aqueous film forming foams (AFFF-AR) and alcohol-resistant fluorine-free foams (FFF-AR) in the past two decades. *Fire Technol.* **2023**, *59*, 429–452. [CrossRef]
16. Zhang, Q.; Wang, L.; Bi, Y.; Xu, D.; Zhi, H.; Qiu, P. Experimental investigation of foam spread and extinguishment of the large-scale methanol pool fire. *J. Hazard. Mater.* **2015**, *287*, 87–92. [CrossRef] [PubMed]
17. Sheng, Y.J.; Li, Y.; Ma, W.Z.; Zhang, H.L. Spreading behavior of firefighting foam solutions on typical liquid fuel surfaces. *J. Surfact. Deterg.* **2022**, *25*, 789–798. [CrossRef]
18. He, Y.H.; Sun, Q.; Xing, H.; Wu, Y.; Xiao, J.X. Cationic-anionic fluorinated surfactant mixtures based on short fluorocarbon chains as potential aqueous film-forming foam. *J. Dispers. Sci. Technol.* **2019**, *40*, 319–331. [CrossRef]
19. Sheng, Y.J.; Jiang, N.; Lu, S.X.; Li, C.H. Fluorinated and fluorine-free firefighting foams spread on heptane surface. *Colloid. Surf. A Physicochem. Eng. Asp.* **2018**, *552*, 1–8. [CrossRef]
20. *GB 15308-2006*; Foam Extinguishing Agent. General Administration of Quality Supervision and Inspection and Quarantine of the People's Republic of China and the Standardization Administration of China: Beijing, China, 2006.
21. Magrabi, S.A.; Dlugogorski, B.Z.; Jameson, G.J. A comparative study of drainage characteristics in AFFF and FFFP compressed-air firefighting foams. *Fire Saf. J.* **2002**, *37*, 21–52. [CrossRef]
22. Hetzer, R.H.; Kümmerlen, F.; Wirz, K.; Blunk, D. Fire testing a new fluorine-free AFFF based on a novel class of environmentally sound high performance siloxane surfactants. *Fire Saf. Sci.* **2014**, *11*, 1261–1270. [CrossRef]
23. Sheng, Y.J.; Jiang, N.; Lu, S.; Wang, Q.; Zhao, Y.; Liu, X. Study of environmental-friendly firefighting foam based on the mixture of hydrocarbon and silicone surfactants. *Fire Technol.* **2020**, *56*, 1059–1075. [CrossRef]
24. Persson, B.; Lönnermark, A.; Persson, H. FOAMSPEX: Large scale foam application—Modelling of foam spread and extinguishment. *Fire Technol.* **2003**, *39*, 347–362. [CrossRef]
25. Persson, B.; Lonnermark, A.; Persson, H. Modelling of foam spread on a burning liquid fuel surface. *Fire Saf. Sci.* **2003**, *7*, 667–678. [CrossRef]
26. Tan, H.L.; Zhang, Y.; Jiang, L.; Zhang, J.Q.; Shang, F.J.; Li, K.Y.; Yang, Y.P. AFFF foam fire extinguishing by gas-permeated spreading and flame barrier with different foaming gases. *Fire Saf. J.* **2025**, *152*, 104330. [CrossRef]
27. White, J.P.; Xin, Y.B. An experimental study of compressed air foam (CAF) protection for ignitable liquid spill fires. *Fire Saf. J.* **2026**, *161*, 104668. [CrossRef]
28. Chen, F.; Gou, H.W.; Tao, J.L.; Cheng, X.D.; He, K. Experimental study on the diffusion characteristics and fire extinguishing effect of foams with different expansion ratios. *Process Saf. Environ. Prot.* **2026**, *208*, 108489. [CrossRef]
29. Bruel, C.; Queffeulou, S.; Darlow, T.; Virgilio, N.; Tavares, J.R.; Patience, G.S. Experimental methods in chemical engineering: Contact angles. *Can. J. Chem. Eng.* **2019**, *97*, 832–842. [CrossRef]

30. Zhao, W.; Xu, Z.; Yan, L. Foaming capability, structural stability, and fire extinguishing performance optimization of short-chain fluorocarbon foam by modulating gas-liquid ratio. *Fire* **2026**, *9*, 59. [CrossRef]
31. Rand, P.B.; Kraynik, A.M. Drainage of aqueous foams: Generation-pressure and cell-size effects. *Soc. Petrol. Eng. J.* **1983**, *23*, 152–154. [CrossRef]

Disclaimer/Publisher's Note: The statements, opinions and data contained in all publications are solely those of the individual author(s) and contributor(s) and not of MDPI and/or the editor(s). MDPI and/or the editor(s) disclaim responsibility for any injury to people or property resulting from any ideas, methods, instructions or products referred to in the content.